PRELIMINARY EVALUATION OF THE NOAA HIGH ENERGY PROTON AND ALPHA-PARTICLE DETECTOR PERFORMANCE

J. B. Blake and W. A. Kolasinski

Space Sciences Laboratory

The Aerospace Corporation

1. Introduction

The purpose of this report is to describe briefly results of testing done at the Brookhaven AGS accelerator and analysis of some on-orbit data acquired from the first two HEPAD flights (TIROS-N and NOAA-6).

The HEPAD (high-energy proton-alpha detector) is designed as a monitor of relativistic, solar-particle fluxes which reach the vicinity of the earth following acceleration at the sun in a solar flare. A detailed description of the HEPAD has been given by Rinehart (1978). The following is a short description for the reader unfamiliar with the sensor configuration. The HEPAD is a three-element counter-telescope consisting of two surface-barrier silicon detectors of 500 microns thickness and a fused-silica Cerenkov radiator which is viewed by a photomultiplier tube. Events which cause coincidences between the three counter elements are analyzed further in terms of signal amplitudes produced in these elements. The HEPAD is mounted on the TIROS satellite so that it continuously points at the zenith; in general, solar particles arrive isotropically distributed over the upper hemisphere.

Relativistic charged particles cause the Cerenkov counter to generate output pulses whose amplitude varies with the particle charge and velocity according to the expression $kZ^2(1-1/\beta^2n^2)$, where Z is the particle charge, k a proportionality constant, β the ratio of the particle velocity to the speed of light and n the index of refraction of the radiator. Thus pulse-height analysis of the Cerenkov counter output gives a measure of the particle energy. Moreover, protons and alpha particles, by virtue of the Z^2 dependence of the pulse amplitude, produce pulses whose amplitudes usually lie in widely different ranges and thus are readily separated by pulse-height analysis. This information, together with measurements of the pulse-height the particle

produces in the two solid-state detectors, is used to identify events to be counted in the alpha-particle channels. Ions heavier than alphas are counted together with the alpha particles since their extremely low abundance relative to protons and alpha particles did not warrant acquiring data in a separate channel(s).

It should be noted that roughly 10% of the proton counts are rejected by virtue of veto signals from the solid-state detectors. These veto signals are generated when amplitude discriminators determine that the signals lie in an amplitude range corresponding to alpha particles. Unfortunately, in the initial design, the contractor overlooked the fact that protons in the Landau tail of the dE/dx curve would be mistaken for alpha particles. By the time this problem had been noticed, it was too late to change the hardware configuration without a major cost and schedule impact and therefore the system was not changed. In Table 1 we give the nominal energy thresholds of the six data channels, and list the various other data channels which are used primarily as diagnostics for checking the sensor performance.

2. Brookhaven Calibration

There were two major objectives behind the tests undertaken at the Brookhaven National Laboratory (BNL) Alternating Gradient Synchrotron (AGS). First and foremost was to answer the unresolved question whether, by using electronic test equipment alone, it is possible to produce copies of a calibrated instrument, with response function to protons and alpha particles matching within required tolerance limits the response function of the calibrated original. An answer to that question was important, since the overall program funding and schedule had been based on the presumption that, after some initial blundering and re-calibrating, a procedure could be

developed to construct instruments which did not require accelerator time for calibration. Extensive testing and calibration had been performed using the proton beam from the Space Radiation Effects Laboratory (SREL) synchro-cyclotron, with a maximum energy of 570 MeV. The major portion of these tests, together with calibration results, has been described by Rinehart (1978). Unfortunately, technical difficulties encountered in the final stages of instrument development, coupled with the permanent shutdown of SREL in the summer of 1978, made it impossible to achieve the above objective.

The second objective of the BNL tests was the removal of an uncertainty in the energy-threshold valves of the P3 and P4 channels. Because of the 570 MeV energy limit imposed by the SREL machine, an indirect method of setting the two high-energy proton thresholds had to be used as described by Rinehart (1978). Inherent in this method is a large uncertainty associated with the actual energy value of these two thresholds and the energy width of the threshold.

The tests at BNL were seheduled to take place during the period 15-19 March 1979, using the AGS A2 Test Beam. Unfortunately the lion's share of the planned test period, already short due to contractor and NASA flight schedules, had to be devoted to becoming acquainted with a totally new test facility. Previously planned test procedures had to be changed to fit constraints imposed by this test facility and not anticipated prior to commencement of testing.

Figure 1 is a functional block diagram of the experimental setup as it evolved during the above mentioned learning period. Crucial in the testing was the time-of-flight (TOF) system shown in Figure 2 consisting of two photomultipliers (PMT's) and associated electronic modules. The PMT's viewing

fast plastic scintillators, approximately 5 cm in diameter and 3 cm thick, were placed approximately 10 m apart along the beam line; the HEPAD telescope axis was aligned with the beam line downstream from the TOF sintillators.

Figure 3 shows in simplified form the electronic system used to combine and process the data from the TOF system and the flight instruments under calibration. The basic approach consisted of setting the TOF window discriminator to bridge the proton peak (the test beam contained pions, muons and some kaons as well as protons). At the same time, all logic pulses from the HEPAD were passed through an active delay of approximately 2 μsec, to arrive at the Logic Interface Module (see Figure 3) slightly delayed with respect to the TOF discriminator signals. The latter were used to gate the interface module and thus prevent the counting of pulses produced in the HEPAD by particles which were not of interest. The analog signals from the two solid state detectors and the Cerenkov detector in the HEPAD, as well as the time to amplitude (TAC) pulses from the TOF system, were passed through appropriate delays in order to be coincident at the multi-channel analyzer (MCA) input and slightly delayed with respect to the various HEPAD and TOF logic pulses. In this way, gated MCA spectra could be readily obtained by selecting any of the four inputs and an appropriate gating signal from the multiple logic unit shown in Figure 3.

In the course of the calibration, desired beam energies or momenta were selected by adjusting the current in a bending magnet to a specified value; the nominal beam energy was checked using the TOF system. Significant deviations of actual beam energies from nominal values were observed. A proton TOF spectrum, obtained by gating the MCA with the window-discriminator output, was saved in one of the MCA quadrants. During most of the scheduled calibration run, HEPAD energy thresholds were measured by obtaining a TOF

spectrum gated by one of the HEPAD proton channels and comparing the result to the spectrum gated by the window discriminator alone. If the proton energy fell near the threshold energy of the p-channel, the spectrum gated by the p-channel would show a large drop in counts within channels corresponding to energies outside the p-channel range. The threshold energy was then determined by the channel at the mid-point of the spectrum "shoulder."

The method of threshold calibration outlined above had the essential drawback that, at the available beam intensity, it was extremely time consuming. Towards the end of the scheduled calibration period a more practical method was developed and used in the calibration of one instrument. This method involved recording counts in all the p-channel scalers at a reasonable number of energies spanning the range of the HEPAD response. Ratios of counts in adjacent channels were then plotted as a function of energy. By definition, the threshold energies are those for which the ratios are equal to unity. Since two channels were needed to determine one threshold by this method, the lowest (P1) threshold still had to be measured by the first technique described. Time remaining in the schedule allowed only one instrument (FM4) to be partially calibrated by the second method.

While leaving much to be desired, the calibrations yielded several important results. The instrument energy thresholds, as measured at BNL, are listed in Table 2. All available instruments were tested, except for FM4, where time did not allow a determination of the P1 threshold. The first conclusion one can draw from the data displayed is that, except for FM4, there is excellent agreement in threshold values from instrument to instrument. It appears therefore that the question posed in the first objective has been answered in the affirmative. With proper care, instrument response functions

can be duplicated to a degree which makes calibration of individual models unnecessary. However, the issue was clouded somewhat by the fact that measured FM4 (and initially FM6) threshold values were drastically different from the nominal ones. In case of FM6, the two sets of values were brought into agreement by adjusting the PMT bias. Presumably the same applies to FM4, but the question remains why were the operating bias commands determined at BNL were lower than those arrived at during calibrations at the contractor's facility. A possible answer lies in a previous observation that during conditions of increased humidity there is a decrease in PMT gain at any given command state. If at any time during calibration by the contractor there had been an unnoticed increase in humidity, the command value determined for the operating high voltage would have been higher than the one found at BNL, where great care was taken to keep the humidity in the HEPAD at zero.

It is clear from Table 2 that while values of the P1, P2 and P3 thresholds are in excellent agreement with the original design values, the measured P4 threshold value is low by approximately 100 MeV. Furthermore, the BNL tests indicate that raising the electronic amplitude threshold results in a considerable decrease in efficiency but only a slight increase in the energy threshold. This result is consistent with a decrease in the light-collection efficiency of the PMT at high proton energy, caused by an opening of the Cerenkov light cone and a resultant increase in the amount of light excaping from the radiator. Further tests need to be performed however to confirm or discredit this hypothesis. In any case, a practical upper limit for the P4 threshold appears to lie in the energy range of 700-750 MeV, and this value had actually been obtained in the laboratory by using the cosmic-ray muons as a calibration source.

The two objectives of the BNL calibrations have been met, albeit not completely. Now that familiarity with the calibration facility exists, a second run of comparable duration would yield much valuable data needed to interpret orbital data of existing instruments and of potential use in design of future instruments. Particularly important is the determination of the angular dependence of the upper two energy thresholds. This dependence appears to be complex due to the sensitivity of the instrument to the angle of the Cerenkov light cone at high energies.

3. On-Orbit Data

Relativistic solar particle events, the phenomena of interest for the HEPAD, are uncommon and exhibit large temporal variations in intensity, spectrum shape and composition. In order to conveniently check the on-orbit performance of the HEPAD it is desirable to observe its response to a stable flux of relativistic ions. There are two such ion populations that can be observed by the HEPAD: the inner-zone protons seen in the vicinity of the South Atlantic Magnetic Anomaly; and the galactic cosmic rays seen over the polar caps. At low latitudes the earth's magnetic field deflects away the lower-energy cosmic rays which are in the energy range of main interest for the HEPAD.

The inner-zone proton fluxes are substantial and can give a HEPAD counting rate of more than 100 counts per 4-second accumulation period. However, these protons do not provide a reliable calibration for several reasons. First, the protons are sharply peaked in a direction normal to the magnetic field, and do not fill the HEPAD 30° half-angle field of view. Furthermore, the pitch-angle distribution of the protons is energy dependent. Finally, the fact that the HEPAD always points at the zenith means

that, in general, the anomaly measurements are not made perpendicular to the magnetic field, and no pitch-angle scan is made. Thus the observed response of the HEPAD to inner-zone protons is complex and it cannot be related easily to the sensor response to isotropic solar-proton fluxes.

The galactic cosmic ray flux is relatively weak and thus one must sum over many polar passes to get adequate counting statistics. On the other hand, cosmic rays do have the desired isotropy and their flux is roughly constant in time, although significant solar-cycle intensity modulation is seen at energies below a couple of GeV. Consequently, the galactic cosmic rays were chosen as a tool for evaluating the HEPAD on-orbit performance.

In Table 3 we show some data from the HEPAD sensors aboard TIROS-N and NOAA-6. The table gives the total counts summed over 50 orbits for TIROS-N from 11 May to 31 May 1979, and over 40 orbits for NOAA-6 from 11 August to 26 August 1979 when the satellites were at values of $L \geq 9$. In Table 4 we give the counting rates for the various HEPAD channels in order that a direct comparison can be made between the sensors aboard the two satellites.

The double coincidences, S5, (cf. Table 1) should be a measure of the integral cosmic ray flux above ~ 65 MeV. Since the photomultiplier tube and its Cerenkov radiator are not involved in this measurement, one would expect that the counting rate in the two sensors to be the same regardless of the performance of the Cerenkov counter. However, the ratio of the NOAA-6 and TIROS-N counting rates in the S5 channel is ~ 1.28 whereas the statistical uncertainty is only a few percent. In an effort to determine the cause of the discrepancy we have plotted in Figures 4 and 5 the observed distribution of the S5 (doubles) counts per 1.2 seconds sample period, along with the expected Poisson distribution for the observed mean rates. It can be seen that NOAA-6

sensor data exhibit an anomalous high-count tail whereas the TIROS-N data look good. If these high-count samples in the NOAA-6 HEPAD data are arbitrarily excluded, a ratio of S5 counting rates of 1.02 is obtained. Thus we conclude that the NOAA-6 sensor has a source of noise which causes some spurious double coincidences.

It also can be noted from the data in Table 2 that the rates in the various channels of the two HEPAD sensors are quite different. In Figure 6 we have plotted these rates converted to a differential flux using the geometric factor of the HEPAD and compare these measurements with the known galactic cosmic-ray flux. It can be seen that the TIROS-N sensor gives results in fair agreement with the known galactic cosmic ray fluxes whereas the NOAA-6 does not. Thus we conclude that the NOAA-6 sensor is not performing properly.

It can be seen that the TIROS-N data show an intensity dip in the second channel. Since we know that in reality no such dip exists, it is concluded that the channel widths are not quite right; the data would fit the cosmic ray spectrum well if the second channel threshold were assumed to be ~ 8% higher. Unfortunately the TIROS-N sensor had not been available for calibration at BNL, or for that matter at SREL, so the question will never be resolved.

The observed alpha particle counting rate is substantially too high. Protons are unquestionally being "promoted" to alpha particles in both the TIROS-N and NOAA-6 HEPADS.

4. Discussion and Recommendations

The above review of HEPAD on-orbit performance has dealt with two instruments (Prototype and FM1) which were not available for calibration at

BNL. One other model, FM3, was also unavailable for the above calibration. Orbital data show that by and large the prototype, flying on the Tiros N satellite, is performing reasonably well. Data from FM1 on the NOAA-6 satellite indicate improper sensor operation, possibly due to the photomultiplier high voltage having been set too high. At the same time, BNL calibrations have shown that in the case of FM6 and probably FM4, high voltage values determined by bench tests at the contractor's facility were incorrect. All of the above facts point to the conclusion that a verification of energy thresholds for every flight instrument should be performed with a real beam of particles, such as the one available at BNL, or at least with the sea-level muon flux.

Three of the HEPAD models are to fly on the GOES spacecraft. Unlike the low, polar TIROS orbits, the synchronous GOES orbit is in an energetic electron environment which will produce a background in the HEPAD data channels. Rinehart (1978) has indicated that the "in-aperture" HEPAD shielding will not stop electrons above ~ 4 MeV. Since the electron environment shows large temporal variations in overall intensity and spectral shape, a knowledge of the HEPAD response to energetic electrons is required for proper interpretation of orbital data. This knowledge also would greatly enhance the usefulness of the HEPAD in that quantitative information about high energy electron environments could be obtained. Such information is needed to make total dose predictions - at present no data exist concerning the electron flux above several MeV.

In view of the above, it is recommended that:

1) At least one HEPAD sensor be calibrated in an energetic electron beam and in the BNL proton beam using a much finer mesh of energy points. Calibration of more than one would add confidence to assumption of identical response.

2) Examine galactic cosmic-ray data soon after each launch to ensure that the photomultiplier high voltage is set properly.

4. Reference

Rinehart, M. C., Cerenkov Counter for Spacecraft Application, Nuc. Inst. Methods, 154, 303, 1978.

TABLE 1

NOMINAL DATA CHANNELS

Channel		Accumulation Interval (seconds)
P1	protons 370-480 MeV	4
P2	protons 480-640 MeV	4
P3	protons 640-970 MeV	4
P4	protons > 970 MeV	4
A1	alphas 640-970 MeV/n	4
A2	alphas > 970 MeV/n	4
S1	solid state detector 1 singles	0.094
S2	solid state detector 2 singles	0.094
S3	Cerenkov singles	0.094
S4	photomultiplier tube gain monitor	2.5
S5	solid state detector doubles (protons > 65 Mev)	1.2

TABLE 2. HEPAD ENERGY THRESHOLDS (IN MEV)

MEASURED AT BNL

MODEL NUMBER	P1 THRESH	P2 THRESH	P3 THRESH	P4 THRESH
FM2	360	460	635	710
FM4	**	<450	524	715
FM5	370	480	630	716
FM6	385	490	630	750
FM7	370	465	625	760

**Not measured due to lack of time.

TABLE 3

HEPAD FLIGHT DATA

Satellite	P1	P2	P3	P4	A1	A2	S1	S2	S3	S4	S5	SAMPLES
TIROS-N	652	519	647	1404	44	89	1465	1481	48819	447087	2448	2671
NOAA-6	493	262	177	1448	85	139	1757	1664	49809	566443	2871	2447

TABLE 4

POLAR CAP FLUXES

Satellite	P1	P2	P3	P4	A1	A2	S5 (doubles)
TIROS-N	6.10(-2)	4.86(-2)	6.06)-2)	1.31(-1)	4.12(-3)	8.33(-3)	7.64(-1)
NOAA-6	5.04(-2)	2.68(-2)	1.81(-2)	1.48(-1)	8.68(-3)	1.42(-2)	9.78(-1)
Ratio of NOAA-6/TIROS-N	.825	.551	.299	1.13	2.11	1.70	1.28

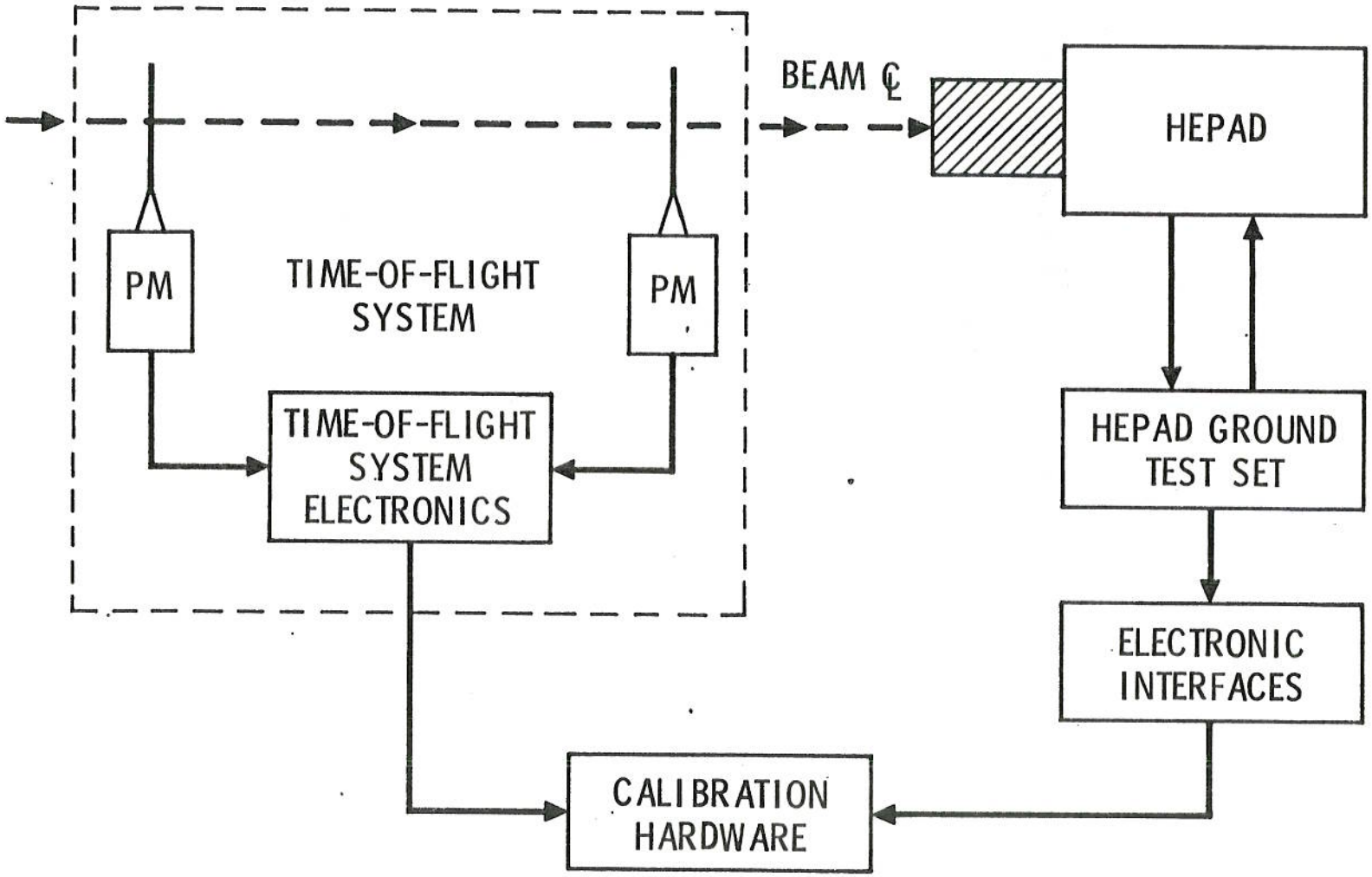

Figure 1 FUNCTIONAL BLOCK DIAGRAM OF TEST ARRANGEMENT

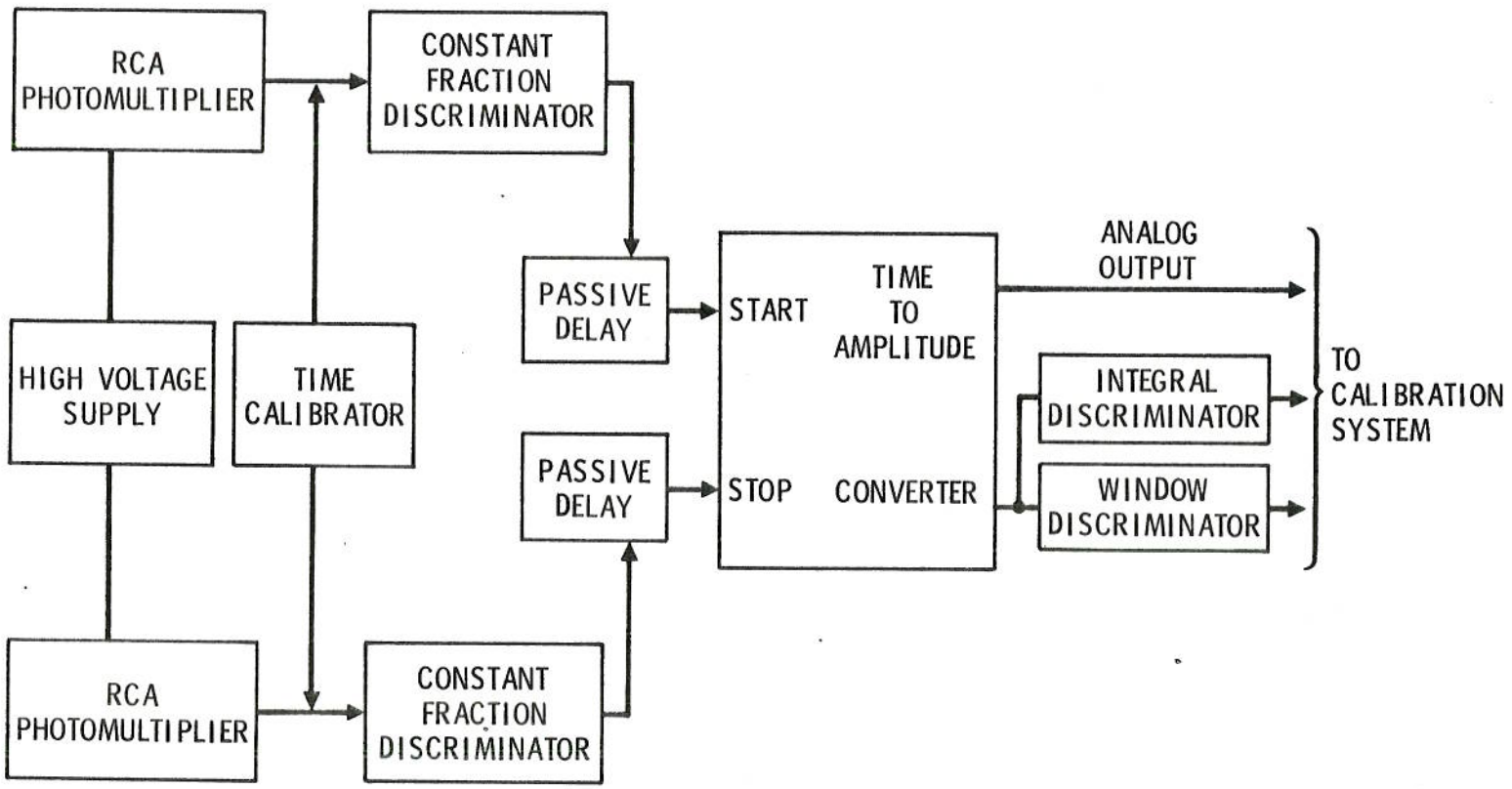

Figure 2 SIMPLIFIED BLOCK DIAGRAM OF TIME-OF-FLIGHT SYSTEM ELECTRONICS

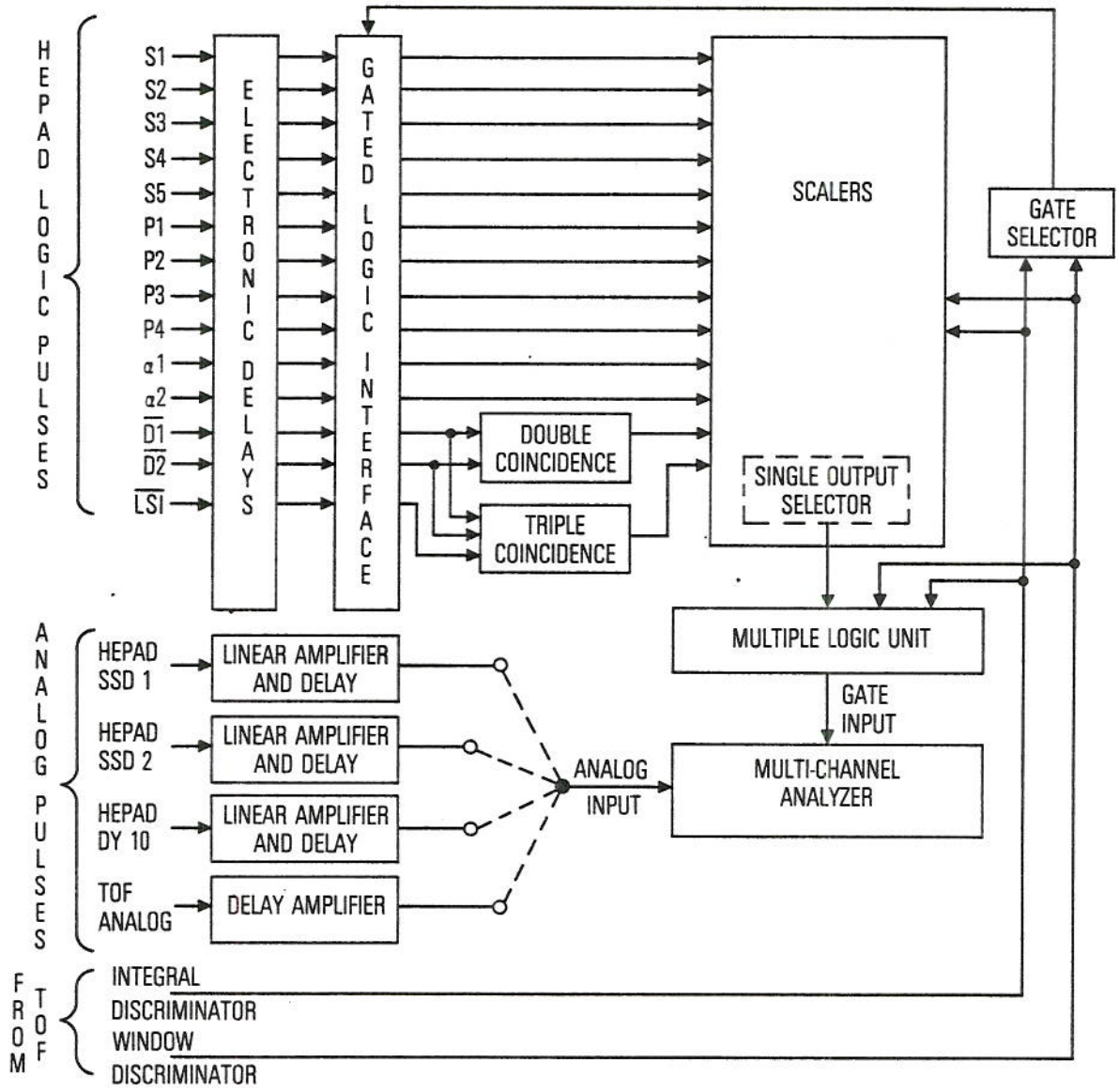

Figure 3 SIMPLIFIED BLOCK DIAGRAM OF HEPAD INTERFACE AND CALIBRATION ELECTRONICS

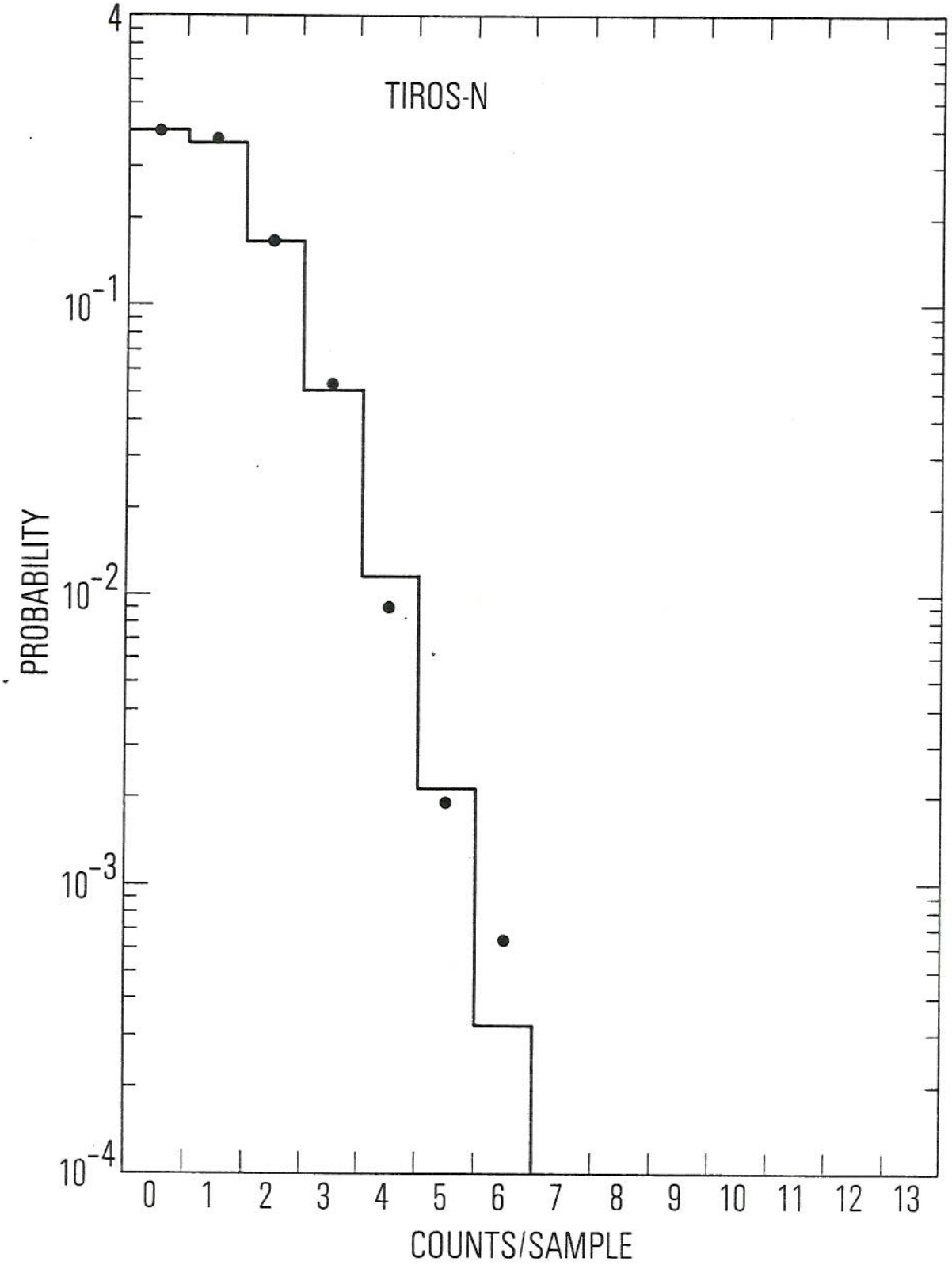

Figure 4 TIROS-N MEASURED COUNTS/INTERNAL DISTRIBUTION COMPARED WITH THE POISSON DISTRIBUTION

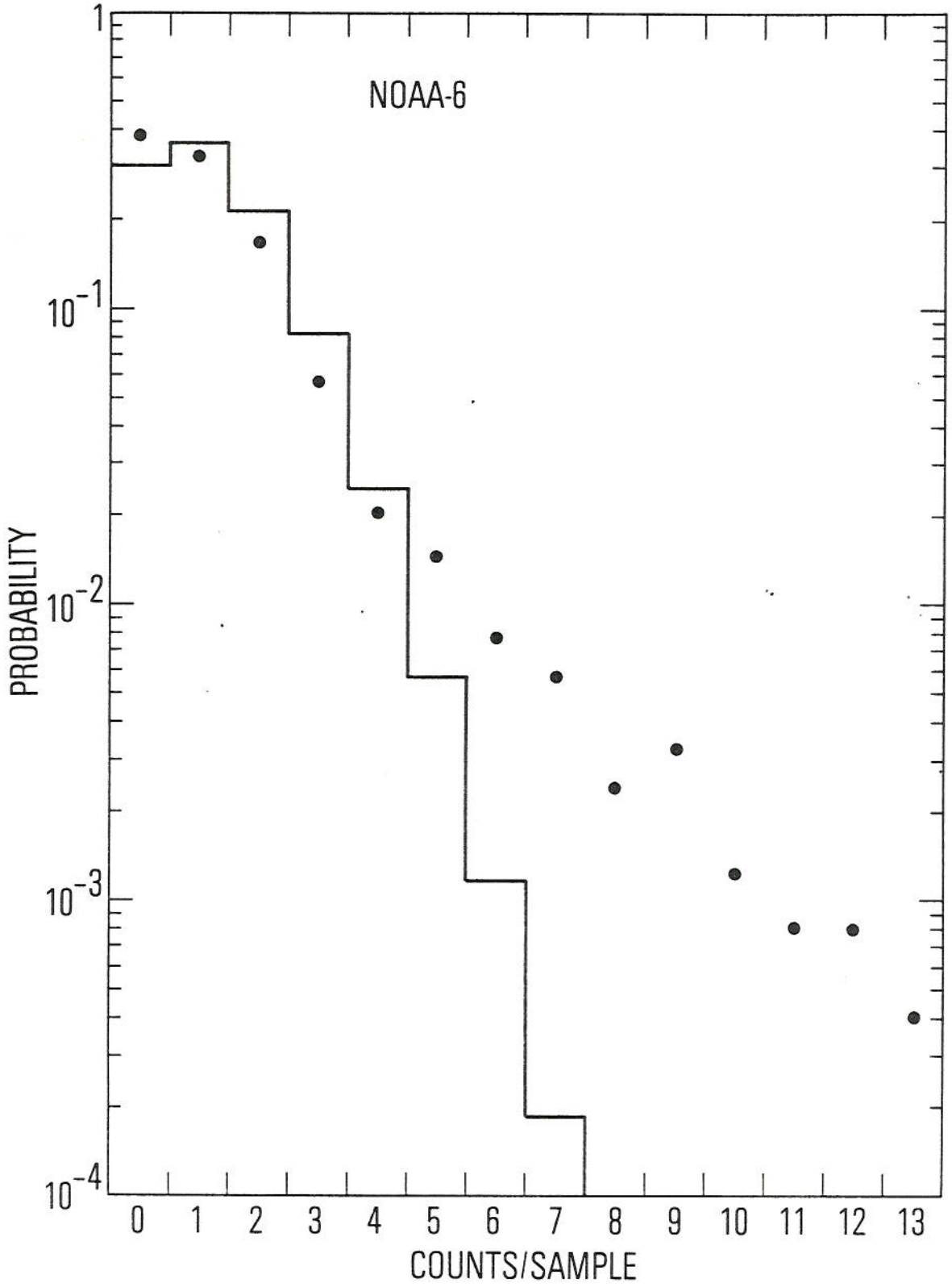

Figure 5 NOAA-6 MEASURED COUNTS/INTERNAL DISTRIBUTION COMPARED WITH THE POISSON DISTRIBUTION

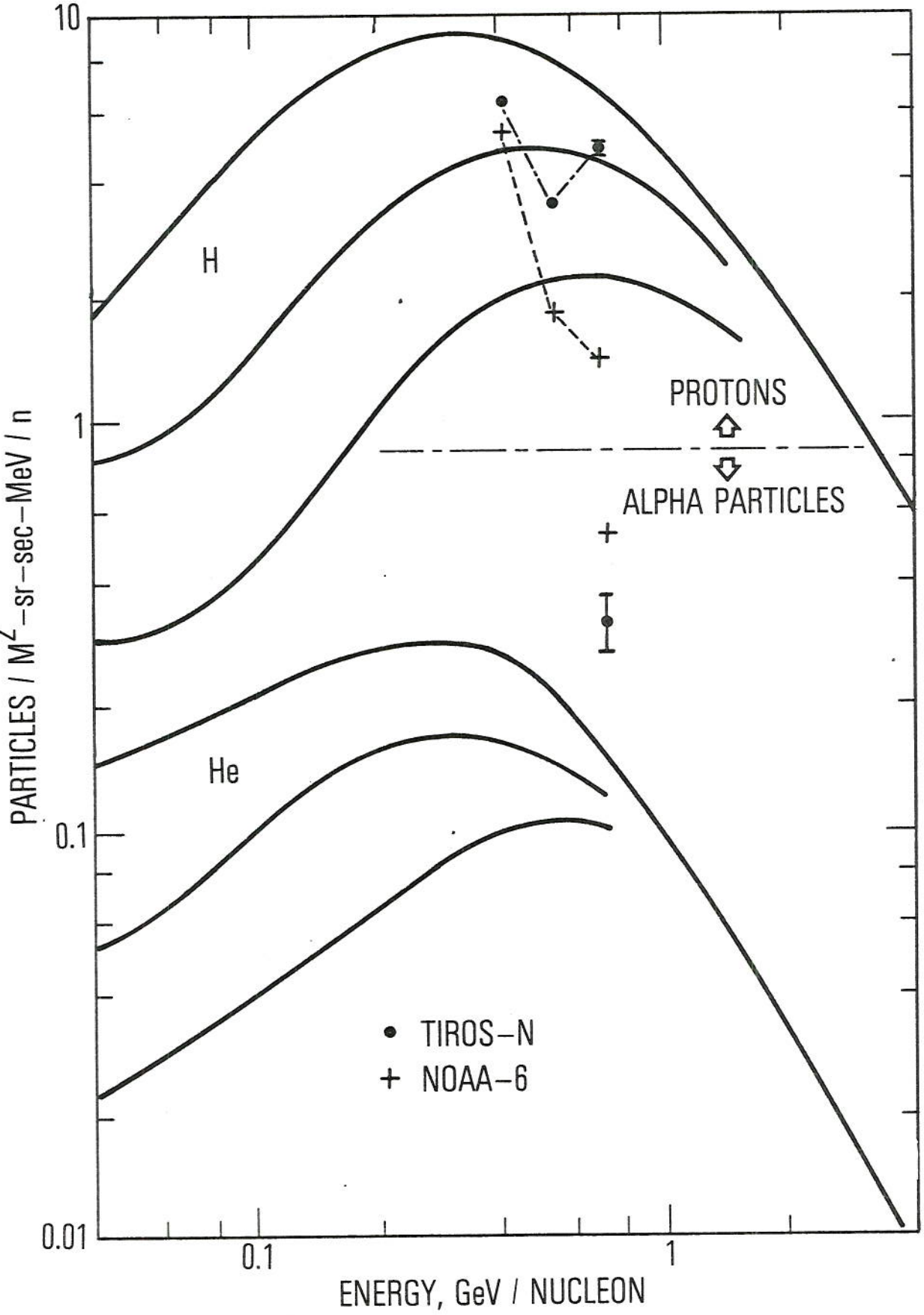

Figure 6 MEASURED PROTON AND ALPHA-PARTICLE FLUXES COMPARED TO KNOWN COSMIC-RAY FLUXES AT DIFFERENT TIMES IN SOLAR CYCLE